MATERIALS SCIENCE AND TECHNOLOGY
2019, VOL. 35, NO. 11, 1301–1305
https://doi.org/10.1080/02670836.2019.1625526

The Institute of Materials, Minerals and Mining

Taylor & Francis
Taylor & Francis Group

CRITICAL ASSESSMENT

Critical Assessment 34: Are χ (Hägg), η and ε carbides transition-phases relative to cementite in steels?

H. K. D. H. Bhadeshia[a], A. R. Chintha[a,b] and S. Lenka[a,b]

[a]Materials Science and Metallurgy, University of Cambridge, Cambridge, UK; [b]Tata Steel Ltd., Mumbai, India

ABSTRACT

Hägg carbide (χ) is, during the tempering of carbon-rich martensite, referred to as a transition carbide which eventually gives way to cementite. However, there are Fe–C binary phase diagrams estimated using thermodynamic data, that define a low-temperature phase field where a mixture of Hägg carbide and ferrite is more stable than that of cementite and ferrite. In this scenario, it may be cementite which is the transition carbide. Evidence is presented here that the predominance of Hägg carbide over cementite in the circumstances described is unlikely to be correct based on historical and new observations. Literature data are also interpreted to show that η and ε-carbides are best regarded as transition-phases relative to mixtures of cementite and ferrite.

ARTICLE HISTORY
Received 8 April 2019
Accepted 27 May 2019

KEYWORDS
Cementite; iron carbides; Hägg carbide; transition carbides; χ-carbide; ε-carbide; η-carbide; Fe–C phase diagram

1. Introduction

There are a number of carbides, other than cementite, in the binary Fe–C system (Table 1). The conventional wisdom of the sequence of precipitation reactions that occur during the tempering of martensite in steels is as follows [1,2]:

$$\alpha' \text{martensite} \rightarrow \underbrace{\varepsilon + \alpha' \rightarrow \eta + \alpha' \rightarrow \chi + \alpha' \rightarrow \theta + \alpha}_{\text{reduction in dissolved carbon} \Longrightarrow} \quad (1)$$

where α′ refers to martensite and α to ferrite. This implies that the first three carbides in this equation form only because there is some kinetic advantage over the more stable cementite.

Chipman [3,4] first contradicted this picture, by suggesting that there is a phase field in the Fe–C equilibrium diagram, where mixtures of χ-carbide and ferrite may be more stable than those of cementite and ferrite, even at the smallest of carbon concentrations. The data utilised to reach this conclusion were based on experiments in which iron was reacted with butane [5]. Based on a single point from these experiments, Chipman derived an admittedly approximate equation for the free energy of formation of χ from α-Fe and graphite, in order to define the χ+α phase field on the Fe–C diagram. Given the uncertainties in the data, he emphasised the need to distinguish thermodynamic and kinetic effects, i.e., whether the experiments on the relative stabilities of χ and θ are sufficiently long to achieve equilibrium.

Given the dearth of data, recent work by Naraghi et al. [6] represented the thermodynamic data for χ and η using data for cementite, but weighted by the composition, for example, by writing the heat capacity at constant pressure as $C_P^{\chi} = \frac{5}{3}C_P^{\theta} + \frac{1}{3}C_{P.}^{\text{graphite}}$ They did not publish the Fe-C phase diagram for temperatures below 900 K, but provided us with the necessary assessed data, resulting in the diagram illustrated in Figure 1. The clear implication is that that χ and η are not always *transition* carbides. The extraordinary outcome is that if a mixture of θ+α is cooled, the cementite would be replaced by χ and eventually, η – the reason why this has never been observed could be kinetic. The purpose of the work presented here was to assess whether such a diagram is viable.

2. First principles calculation data

Ab initio calculations of individual crystals are often taken to be indicative of an order of thermodynamic stability. Table 2 lists the change in internal energy when each of the carbides is formed from elemental iron and carbon. In making comparisons, a larger ΔU corresponds to a lower stability. The data reported by Faraoun et al. [15] are abnormally large; the space group quoted for cementite by Faraoun et al. is inconsistent with the lattice parameters assumed, and the η-carbide unit cell seems to have a *c*-parameter that is larger than *a* or *b*, whereas the opposite is in fact true; these data are therefore ignored. The discrepancies within the other data are nevertheless sufficiently large

CONTACT H. K. D. H. Bhadeshia hkdb@cam.ac.uk Materials Science and Metallurgy, University of Cambridge, 27 Charles Babbage Road, CB3 0FS Cambridge, UK

Table 1. Iron carbides.

Carbide	Approximate composition	Space group
Cementite θ	Fe_3C	Orthorhombic *Pnma*
ε-carbide	$Fe_{2.4}C$	Hexagonal $P6_3/mmc$ or $P6_322$
χ-carbide	$Fe_{2.2}C$	Monoclinic *C2/c*
η-carbide	Fe_2C	Orthorhombic *Pnnm*

Note: The actual composition of ε-carbide can affect its crystal structure, hence the two space groups.

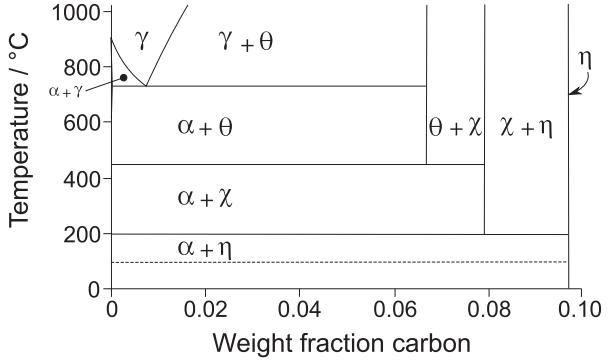

Figure 1. Part of the iron-carbon equilibrium phase diagram calculated using data provided by Naraghi et al. [6]. The dashed line represents a temperature below which a solid solution of iron and carbon may tend to undergo the clustering of carbon atoms as a precursor to a conditional spinodal.

Table 2. First principles calculations of the change in internal energy ΔU at 0 K and zero pressure for the reaction $\Delta U = [U_{Fe_nC_m} - nU_{Fe} - mU_C]/(n+m)$.

Carbide	ΔU / kJ mol^{-1}	Reference
Cementite Fe_3C	5.38	[7–9]
Cementite Fe_3C	5.89	[10]
Cementite Fe_3C	5.60	[11]
Cementite Fe_3C	5.21	[11]
Cementite Fe_3C	2.51	[12]
ε-carbide $Fe_{2.4}C$	6.23	[13]
ε-carbide $Fe_{2.2}C$	4.26	[14]
η-carbide Fe_2C	126.1	[15]
η-carbide Fe_2C	4.00	[14]
η-carbide Fe_2C	1.68	[12]
Häag χ-carbide Fe_5C_2	152.6	[15]
Häag χ-carbide Fe_5C_2	2.45	[12]

Note: These are calculations that consider the formation of the carbide as an isolated phase, from the constituent atoms.

to make the relative stabilities of the carbides difficult to assess with confidence. Furthermore, the calculations are representative of 0 K and zero pressure, whereas the formation energies are in fact sensitive to temperature (Figure 2) [10,16]. Temperature-dependent calculations that account for magnetic and other heat capacity terms, show that η-carbide is less stable than cementite beyond 57°C [17].

3. Observations of χ, η, ε and θ carbides in tempered Fe-C

Table 3 summarises the data assembled from a search of the literature, for plain carbon steels (Fe–C) which have been tempered from a supersaturated-ferritic or martensitic condition. The number of observations is small, but not surprising given that Fe–C binary steels are not commercially viable. The data include the

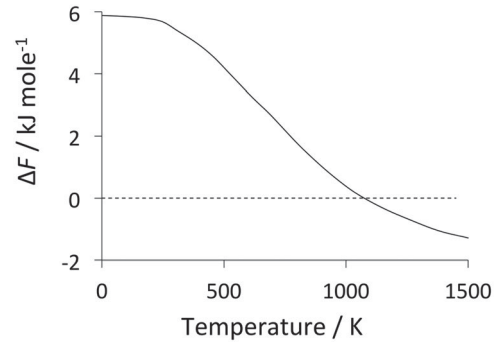

Figure 2. The formation energy ΔF of cementite for the reaction $F_{Fe_3C} - [3F_{Fe} + F_{graphite}]/4$. Data from CALPHAD assessment by Hallstedt et al. [10]. A negative value implies that cementite becomes stable relative to the mixture of α and graphite.

Table 3. Fe-C steels (neglecting trace impurities) in which carbides have precipitated during tempering of supersaturated ferrite or martensite.

Carbide	Steel / wt-%	Heat treatment	Reference
χ	Fe-1.22C	300°C, 350°C, 1 h	[18]
χ	Fe-1.5C	277°C, 48 h	[19]
η	Fe-1.13C	120°C, 1–100 days	[20]
η	Fe-1.22C	125°C, 16 h	[21]
ε	Fe-1.3C	120°C, 960 h	[22]
ε	Fe-0.8C	204°C, 1 h; 260°C, 1 h	[23]
ε	Fe-1.80C	73°C, 240 h	[24]
ε	Fe-0.81C	125°C, 1 h	[25]
θ	Fe-0.02C	250°C, 15–250 min	[26]
θ	Fe-0.014C	150°C, 170 h; 260°C, 3–10 min	[27]
θ	Fe-0.8C	316°C, 1 h	[23]
θ	Fe-0.8C	427°C, 1 h	[23]
θ	Fe-1.30C	350°C, 21 d	[22]

Note: The very low carbon data represent cases where allotriomorphic ferrite was quenched and then tempered.

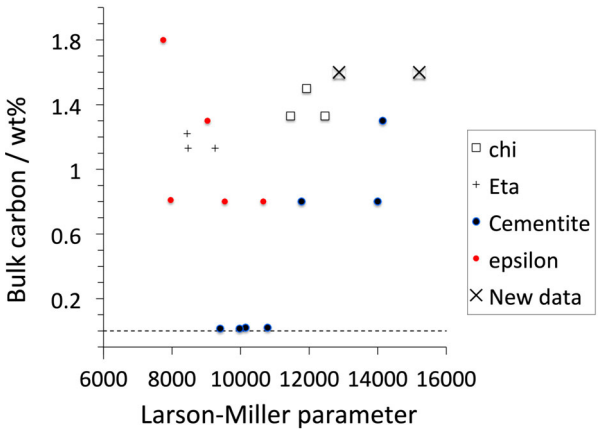

Figure 3. Plot of the data presented in Table 3, against a Larson–Miller parameter $T(\log t + 20)$, where T is the absolute tempering-temperature and t the tempering time in hours. The new data describe cementite obtained from our own tempering experiments as described below.

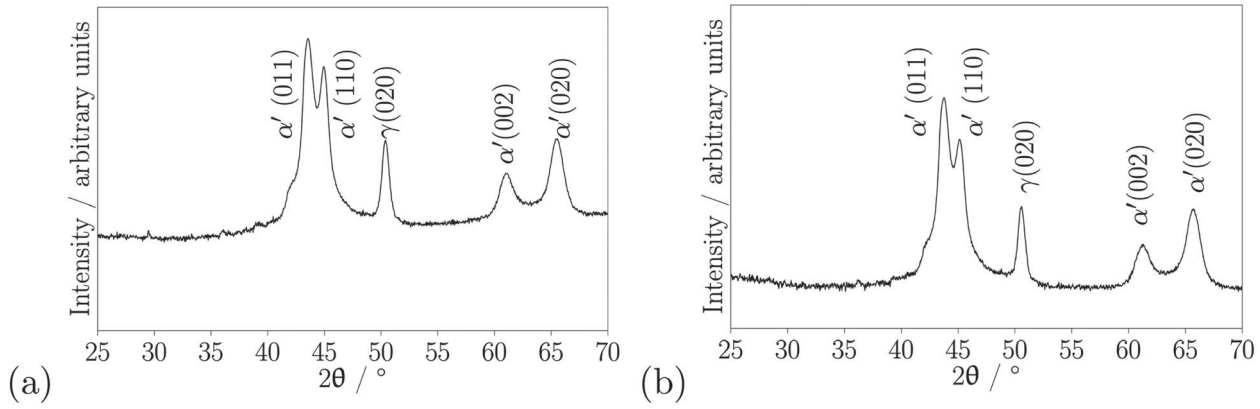

Figure 4. X-ray diffraction data from quenched and cryogenically treated samples of Fe-1.60C wt-%. (a) Sample A, containing 0.11±0.01 volume fraction of retained austenite. (b) Sample B also containing 0.11±0.01 volume fraction of retained austenite.

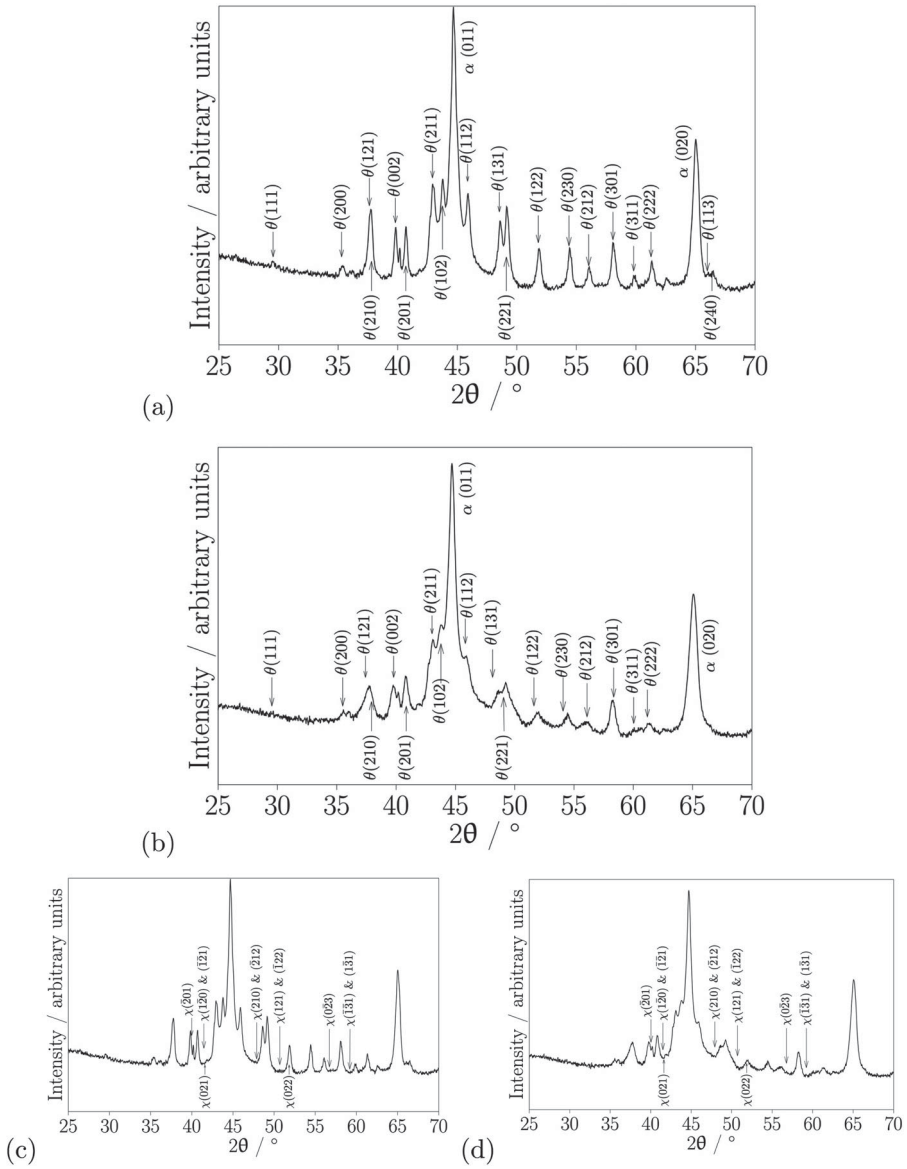

Figure 5. X-ray diffraction data from the tempered samples of Fe-1.60C wt-%. (a) Sample A, tempered at 400°C. The small peak at 62.5° could not be identified with any of the carbide or matrix phases (b) Sample B, tempered at 300°C. The same data were then used to check against χ-carbide: (c) Sample A, tempered at 400°C. (d) Sample B, tempered at 300°C.

tempering temperatures and times. With one exception, the tempering times involved are probably not sufficient for the system to equilibrate and permit χ, η and ε to transform into θ. Figure 3 represents a plot of these data, using a Larson–Miller parameter [28] to represent the *kinetic strength* of the heat treatment. Although empirical, the parameter is acknowledged widely to rationalise the combined effects of time and temperature during tempering [e.g. 29–31]

Two conclusions can be drawn from Figure 3. First, that cementite seems to be the most stable phase over a wide temperature range when the strength of the heat treatment is greatest within the scope of the dataset. Second, that cementite is the only precipitate when the excess carbon concentration is very small. This would be expected for a phase of high stability because a small carbon concentration in solution corresponds to a small driving force for precipitation. In such circumstances, transition phases (which by definition lead to a smaller reduction in free energy) would not be able to precipitate.

4. Experiments

An arc melted 60 g sample made from pure electrolytic-iron and carbon was made and chemically analysed to have the composition Fe-1.60 wt-%. Two samples were sealed in quartz tubes for austenitisation at 1120°C for 1 h before quenching into water. Because of the large carbon concentration, to promote further martensitic transformation, the samples were cooled into liquid nitrogen. Sample A was kept there for 27 h, and sample B for 36 h; the difference is simply a consequence of practicalities.

Both were then subjected to X-ray diffraction covering $2\theta = 25–70^\circ$ with a step size of 0.03° and a dwell time of 15 s. The measurements used nickel-filtered CuK_a radiation and the data were subjected to Reitveld refinement. Sample A was then sealed in a glass tube and tempered at 400°C for 406 h (Larson–Miller parameter 15216) and Sample B at 300 for 295 h (Larson–Miller parameter 12875), after which they were once again subjected to X-ray analysis.

The quenched samples exhibited only martensite and retained austenite, Figure 4. In contrast, the patterns presented in Figure 5(a,b) show that for both tempering temperatures, the austenite has vanished and peaks that can with clarity be indexed to cementite are present. The volume fractions of cementite were measured to be 0.237 ± 0.001 and 0.24 ± 0.002 in Samples A and B, respectively. These compare very well with the equilibrium fractions estimated using phase diagram calculations (allowing only cementite and ferrite to exist), for both tempering temperatures, at 0.239. No evidence of χ carbide could be found in either case; Figure 5(c,d) shows the same patterns separately, but with the positions where the strongest of χ peaks are expected. It is evident that there is no χ-carbide present. The two crosses marked onFigure 3 therefore represent cementite.

5. Summary

An investigation of literature data and our own experiments establish that it is not correct to identify a $\chi+\alpha$ phase field on the iron-carbon equilibrium phase diagram (Figure 1), one which is supposed to be more stable than $\theta+\alpha$. Furthermore, the analysis of published data indicates that the $\eta+\alpha$ phase field on Figure 1 is also unlikely to be correct because only cementite is observed to form in very low carbon steels at low tempering temperatures. The conclusion is that the thermodynamic data on which the phase diagram calculations are based need further probing.

Acknowledgments

Harry Bhadeshia is grateful to Professor J. Ågren for his prompt response to queries and for providing the thermodynamic data [6] used in the calculation of the Fe–C phase diagram. Apparao Chintha and Shaumik Lenka are grateful to Tata Steel Ltd. India for funding their research in Cambridge.

Disclosure statement

No potential conflict of interest was reported by the authors.

References

[1] Dirand M, Afqir L. Identification structural precise des carbures precipites dans lest aciers faiblement allies aux divers stades due revenu. Mechanismes de precipitation. Acta Metallurgica. 1983;31:1089–1107.
[2] Jack DH, Jack KH. Carbides and nitrides in steel. Mater Sci Eng. 1973;11:1–27.
[3] Chipman J. Thermodynamics and phase diagram of the Fe-C system. Metall Trans. 1972;3:55–64.
[4] Chipman J. Metals handbook, Hawkins D. T. and Hultgren R., editors. vol. 8, chap. C-Fe: Metals Park (OH): American Society for Metals; 1973. p. 277–278.
[5] Browning LC, DeWitt TW, Emmett PH. Equilibria in the systems Fe_2C-Fe-CH_4-H_2 and Fe_3C-Fe-CH_4-H_2. J Am Chem Soc. 1950;72:4211–4217.
[6] Naraghi R, Selleby M, Ågren J. Thermodynamics of stable and metastable structures in the Fe-C system. Calphad. 2014;46:148–158.
[7] Jang JH, Kim IG, Bhadeshia HKDH. Substitutional solution of silicon in cementite: a first-principles study. Comput Mater Sci. 2009;44:1319–1326.
[8] Jang JH, Kim IG, Bhadeshia HKDH. First-principles calculations and the thermodynamics of cementite. Mater Sci Forum. 2010a;638-642:3319–3324.
[9] Kim IG, Rahman G, Jang JH, et al. A systematic study on iron carbides from first principles. Mater Sci Forum. 2010;654-656:47–50.
[10] Hallstedt B, Djurovic D, von Appen J, et al. Thermodynamic properties of cementite (Fe_3C). Calphad. 2010;34:129–133.
[11] Konyaeva MA, Medvedeva NI. Electronic structure, magnetic properties and stability of binary and ternary

$(Fe,Cr)_3C$ and $(Fe,Cr)_7C_3$. Phys Solid State. 2009;51: 2084–2089.
[12] Fang CM, van Huis MA, Zandbergen HW. Stability and structures of the ε-phases of iron nitrides and iron carbides from first principles. Scr Mater. 2011;64:296–299.
[13] Jang JH, Kim IG, Bhadeshia HKDH. ε-carbide in alloy steels: first-principles assessment. Scr Mater. 2010b;63:121–123.
[14] Liu XW, Cao Z, Zhao S, et al. Iron carbides in Fischer-Tropsch synthesis: theoretical and experimental understanding in epsilon-iron carbide phase assignment. J Phys Chem C. 2017;121:21390–21396.
[15] Faraoun HI, Zhang YD, Esling C, et al. Crystalline, electronic, and magnetic structures of θ-Fe_3C, χ-Fe_5C_2, and η-Fe_2C from first principle calculation. J Appl Phys. 2006;99:093508.
[16] Bhadeshia HKDH. 'Cementite', Int Mater Rev, 2019;64. https://doi.org/10.1080/09506608.2018.1560984
[17] Fang CM, Sluiter MHF, van Huis MA, et al. Origin of predominance of cementite among iron carbides in steel at elevated temperatures. Phys Rev Lett. 2010;105:055503.
[18] Ma CB, Ando T, Williamson DL, et al. Chi-carbide in tempered high carbon martensite. Metallurgical Mater Trans A. 1983;14:1033–1045.
[19] Nakamura Y, Mikami T, Nagakura S. *In situ* high temperature electron microscopic study of the formation and growth of cementite particles in the third stage of tempering. Trans Japan Inst Metals. 1985;26: 876–885.
[20] Hirotsu Y, Nagakura S. Crystal structure and morphology of the carbide precipitated from martensitic high-C steel during the 1st stage of tempering. Acta Mater. 1972;20:645–655.
[21] Williamson DA, Nagazawa S, Krauss G. A study of the early stages of tempering in an Fe-1.2C pct alloy. Metall Trans A. 1979;10:1351–1363.
[22] Jack KH. Structural transformations in the tempering of high-carbon martensitic steels. J Iron Steel Inst. 1951;169:26–36.
[23] Austin AE, Schwartz CM. Electron- diffraction study of iron carbides in bainite and tempered martensite. Proc ASTM. 1952;52:592–596.
[24] Okamoto H, Oka M. Isothermal martensite transformation in a 1.80 wt% C steel. Metall Mater Trans A. 1985;16:2257–2262.
[25] Murphy S, Whiteman JA. The precipitation of epsilon-carbide in twinned martensite. Metall Trans. 1970;1: 843–848.
[26] Langer EW. An investigation of carbide precipitation in iron. Metal Sci J. 1968;2:59–66.
[27] Leslie WC, Fisher RM, Sen N. Morphology and crystal structure of carbides precipitated from solid solution in alpha iron. Acta Metall. 1959;7:632–644.
[28] Larson FR, Miller J. Time-temperature relationships for rupture and creep stresses. Trans ASME. 1952;74: 765–781.
[29] Heimerl GJ. 'Time-temperature parameters and an application to rupture and creep of aluminum alloys'. Washington (DC): National Advisory Committee for Aeronautics; 1954. (Tech. Rep. 3195).
[30] Canale LC, Yao X, Gu J, et al. A historical overview of steel tempering parameters. Int J Microstruct Mater Properties. 2008;3:474–525.
[31] Virtanen E, Tyne CJV, Levy BS, et al. The tempering parameter for evaluating softening of hot and warm forging die steels. J Mater Processing Technol. 2013;213:1364–1369.